Silicon Microtoroidal Resonators with Integrated MEMS Tunable Optical Coupler

Jin Yao[1], David Leuenberger[1], Ming-Chang M. Lee[2], and Ming C. Wu[1]
[1]*Berkeley Sensor & Actuator Center (BSAC) and Dept. Electrical Engineering and Computer Sciences, University of California, Berkeley, California 94720, USA*
Tel: (510) 643-5801, Fax: (510) 643-5817, Email: jinyao@eecs.berkeley.edu
[2]*Dept. Electrical Engineering & Institute of Photonics Technologies, National Tsing Hua University, HsinChu, Taiwan, 30055, ROC*

Abstract— A single crystalline silicon microtoroidal resonator with integrated MEMS tunable optical coupler is demonstrated for the first time. The coupling coefficient is continuously tuned from almost zero up to 13.3%.

I. INTRODUCTION

Optical microresonators are key enabling elements for compact modulators [1], filters [2], optical delay lines [3], nonlinear optical devices [4], and optical sensors [5]. The performance of microresonators depends on two critical parameters: the quality factor (Q) and the power couple ratio between the waveguides and the resonator (κ). The ability to control κ is important to optimize the performance of microresonator circuits. It also enables dynamically tunable or reconfigurable devices. While it is possible to vary κ by bulk micropositioners in hybrid devices with external fiber couplers [4,5], most integrated microresonators have fixed κ [1-3]. Previously, we have reported the first silicon *microdisk* resonator with integrated tunable coupler, and demonstrated a tunable dispersion compensator [6].

In this paper, we report on the first *single crystalline silicon microtoroidal* resonator with MEMS tunable coupler. Microtoroidal resonators offer tighter confinement of the optical mode and eliminate multiple radial modes observed in microdisks. Microtoroidal SiO_2 resonators have been made by thermal reflow [7], however, such process cannot be applied to single crystalline structures. Previously, we have demonstrated the use of hydrogen annealing to create the 3-D toroidal structure while preserving the single crystalline quality [8]. Here, we combine the hydrogen annealing with wafer bonding process to integrate microtoroidal resonators with MEMS tunable waveguides. High performance resonator with a Q of 110,000 has been achieved.

II. DEVICE DESIGN AND FABRICATION

The schematic of the tunable microtoroidal resonator is shown in Fig. 1. It is realized on a two-layer silicon-on-insulator (SOI) structure. The microtoroid and the fixed electrodes of the MEMS actuator are realized in the lower SOI layer, while the vertically coupled deformable waveguides are fabricated on the upper SOI. The initial spacing (1 μm) is chosen so that there is negligible coupling at zero bias. With increasing voltage bias, the suspended waveguide is pulled down towards the microtoroid, increasing the coupling exponentially. As will be shown later, we are able to bias the waveguide in all three coupling regimes: under-coupling, critical coupling, and over-coupling.

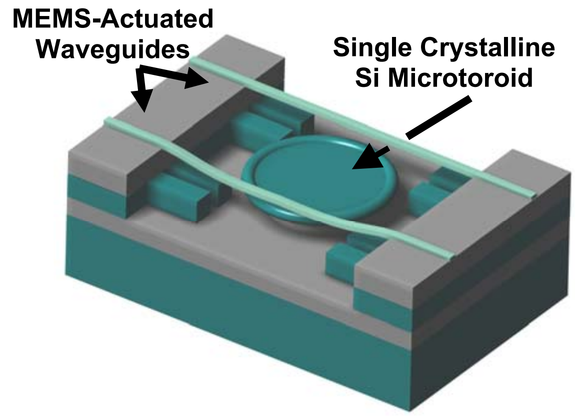

Figure 1. Schematic of the microtoroidal resonator with integrated MEMS tunable couplers. The left waveguide is pulled downward to increase coupling, while the right waveguide remains flat (uncoupled).

The fabrication process (Fig. 2) is described in the following. First, microdisks are patterned on an SOI wafer with 350nm-thick device layer. The edges of the disks are thinned down to 200 nm. The sample is then partially released and annealed in 10 Torr hydrogen ambient at 1050°C for 5 minutes, creating toroidal rims around the disks [8]. The toroidal wafer is fusion bonded to another SOI wafer, whose substrate is subsequently removed to reveal the second SOI layer. Waveguides patterns are aligned to the underneath microtoroids. Finally, the waveguides around the toroids are released in buffer HF and supercritical dryer. In addition to creating toroidal shape, the hydrogen annealing also greatly reduces the surface roughness (to < 0.26 nm [8]).

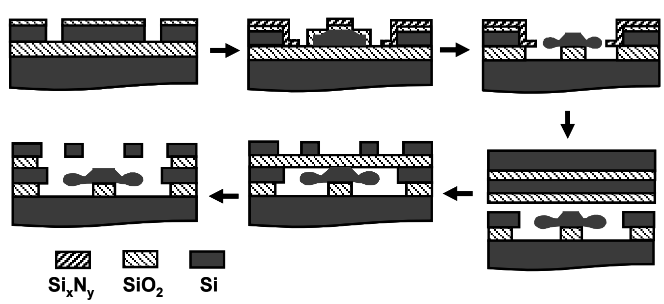

Figure 2. Fabrication processes of the tunable microtoroidal resonator.

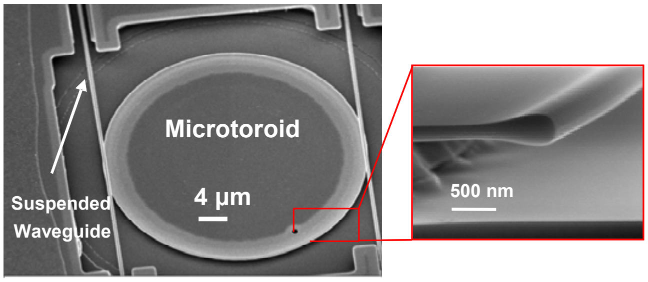

Figure 3. The SEM of a fabricated device. The inlet shows the cross-sectional profile of the microtoroid. The toroidal radius is 200 nm.

The scanning electron micrograph (SEM) of the fabricated device is shown in Fig. 3. The resonator has a ring radius of 19.5μm and a toroidal radius of 200 nm. Phase matching between the waveguide and the microtoroid is achieved by properly controlling the dimension of the waveguides (0.7μm wide and 0.26μm thick).

III. Optical Characterization

The tunable microtoroidal resonator is tested using a broadband amplified spontaneous emission (ASE) source under various bias conditions. Light is coupled to the waveguides through polarization maintaining lensed fibers. The spectral response is shown in Fig. 4. At zero bias, almost 100% of light is transmitted to the output port. With increasing bias, the transmittance at the resonant wavelength (1548.18 nm) gradually decreases. At an actuation voltage of 64.8 V, the extinction ratio reaches 10.2 dB. The coupling coefficient can be extracted by fitting the experimental curve with the model based on time-domain coupling theory [2]. The κ can be continuously varied from zero (negligible coupling) to 13.3%.

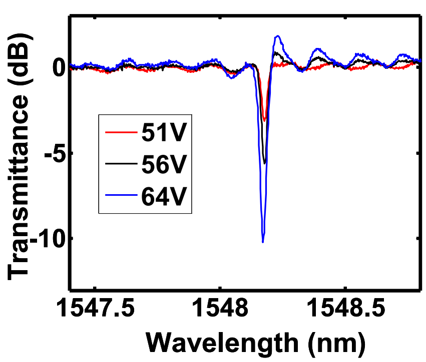

Figure 4. Measured spectra of the microtoroidal resonator under various bias voltages.

The spectral response over a wider wavelength range is shown in Fig. 5. The free spectrum range (FSR) of the TE mode is measured to be 5.2 nm. The small ripples are due to the reflections from the cleaved facets (Fabry-Perot effect). Only one resonance peak is observed within one FSR, confirming the successful suppression of multiple radial modes observed in microdisk resonators.

The inset of Fig. 5 shows the measured and the modeled spectral response around the resonant peak at 1548 nm. From the fitted spectral response, the unloaded Q of the microtoroid is estimated to be 110,000. The high quality factor confirms the smooth surface of the microtoroid produced by hydrogen annealing process.

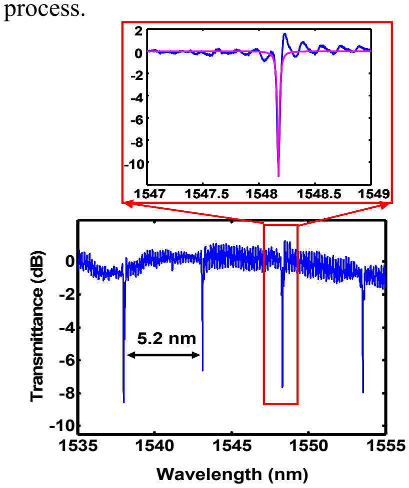

Figure 5. Optical spectrum over the 1550 nm regime and the detailed spectrum around the resonance at 1548 nm. The blue and the red line in the inlet represent the experimental data and the fitting, respectively.

IV. Summary

We have successfully demonstrated a single crystalline silicon microtoroidal resonator with MEMS-actuated tunable optical coupler. It is fabricated by combining the hydrogen annealing and the wafer bonding processes. We have achieved an unloaded Q of 110,000 for a 39-μm-diameter resonator with a toroidal radius of 200 nm. The coupling coefficient is continuously tunable from almost zero to 13.3%. This device has potential applications in variable bandwidth filters, reconfigurable optical add-drop multiplexers, and optical sensors. This project is supported in part by DARPA UPR Program HR0011-04-1-0040.

References

[1] Q. Xu, et al., "Micrometre-scale silicon electro-optic modulator," *Nature*, vol. 435, no. 7040, pp. 325-327, May 2005.

[2] B.E. Little, et al., "Microring resonator channel dropping filters," *Journal of Lightwave Technology*, vol. 15, no. 6, pp. 998-1005, Jun. 1997.

[3] G. Lenz, et al., "Optical delay lines based on optical filters," *IEEE Journal of Quantum Electronics*, vol.37, pp. 525-32, Apr. 2001.

[4] T.J. Kippenberg, et al., "Ultralow-threshold microcavity Raman laser on a microelectronic chip," *Optics Letters*, vol. 29, pp. 1224-6, June 2004.

[5] F. Vollmer, et al., "Multiplexed DNA Quantification by Spectroscopic Shift of Two Microsphere Cavities," *Biophysical Journal*, vol.85 pp.1974–1979, September 2003.

[6] MC. Lee, et al., "MEMS-Actuated Microdisk Resonators with Variable Power Coupling Ratios," *IEEE Photonics Technology Letters,* vol. 17, pp.1034-1036, May 2005.

[7] D.K. Armani, et al., "Ultra-high-Q toroid microcavity on a chip", *Nature*, vol. 421, pp. 925-929, Feb. 2003.

[8] MC. Lee, et al., "Silicon Profile Transformation and Sidewall Roughness Reduction Using Hydrogen Annealing," in *18th IEEE International Conference on Micro Electro Mechanical Systems*, 2005, pp. 596-9.